Cell, Vol. 82, 19–28, July 14, 1995, Copyright © 1995 by Cell Press

Overexpression of the Hyaluronan Receptor RHAMM Is Transforming and Is Also Required for H-*ras* Transformation

Christine L. Hall,* Baihua Yang,* Xuiwei Yang, Shiwen Zhang, Maureen Turley, Shanti Samuel, Laurie A. Lange, Chao Wang, Genevieve D. Curpen, Rashmin C. Savani, Arnold H. Greenberg, and Eva A. Turley
Manitoba Institute of Cell Biology
and Department of Pediatrics
University of Manitoba
Winnipeg, Manitoba R3E 0V9
Canada

Summary

Overexpression of the RHAMM gene by transfection into fibroblasts is transforming and causes spontaneous metastases in the lung. H-*ras*-transformed fibrosarcomas transfected with a dominant suppressor mutant of RHAMM exhibit a so-called revertant phenotype and are completely nontumorigenic and nonmetastatic. Conversely, fibroblasts stably expressing low levels of RHAMM as a result of antisense transfection are resistant to *ras* transformation. Collectively, these results indicate that RHAMM acts downstream of *ras*. The loss of functional RHAMM ablates signaling within focal adhesions, in particular changes in focal adhesion kinase phosphorylation, and as a result these focal adhesions are unable to turn over in response to hyaluronan. These results provide evidence of the oncogenic potential of a novel extracellular matrix receptor and establish a functional link between transformation by *ras* and signaling within focal adhesions that are required for transformation by this oncogene.

Introduction

Extracellular matrix (ECM) molecules, their receptors, and gene products that modify the ECM are able to influence directly cell characteristics such as growth and motility (Ratner, 1992; Damsky and Werb, 1992; Hynes, 1992; Ruoslahti et al., 1994; Lin and Bissell, 1993; Jones et al., 1993), to regulate cellular responses to growth factors and cytokines (Noble et al., 1993; Chong et al., 1992; Hiro et al., 1986), and to modify the transformed state. Many of these ECM receptors and their ligands can regulate the invasive/metastatic phenotype in tumorigenic cells. Thus, overexpression of α4β1 integrin inhibits invasion during metastasis (Qian et al., 1994), while overexpression of the urokinase receptor enhances invasion (Kariko et al., 1993). A regulator of metalloproteinases, TIMP-1, inhibits invasion of metastatic cells (Khokha et al., 1992; Alexander and Werb, 1992). Other ECM receptors, however, partially modify the transformed state of cells. Thus, α5β1 integrins partially restore contact inhibition and anchorage-dependent growth properties of the tumorigenic CHO cells (Giancotti and Ruoslahti, 1990), while overexpression of thrombospondin (Castle et al., 1993) results in the development of serum-independent growth. However, none of these ECM receptors has been frankly shown to be transforming.

The receptor for hyaluronan-mediated motility (RHAMM) signals elevated cell locomotion via a transient tyrosine phosphorylation within focal adhesions that results in their turnover in *ras*-transformed cells (Hall et al., 1994). RHAMM is regulated by growth factors such as transforming growth factor β1 (TGFβ1), and its expression is necessary for TGFβ1 stimulation of fibrosarcoma cell motility (Samuel et al., 1993). We show here that, in contrast with other ECM receptors, overexpression of the hyaluronan (HA) receptor RHAMM (Hardwick et al., 1992) is both transforming and able to generate a metastatic phenotype, in which the subcutaneous tumors of RHAMM-transfected cells spontaneously metastasize, and these cells also form lung colonies after inoculation in the tail vein. The ability of RHAMM to transform fibroblasts indicates that this receptor functions in a fundamentally different manner than other characterized ECM receptors. In view of the elevated expression of RHAMM in *ras*-transformed cells (Turley et al., 1991) and its importance in the locomotion of these cells (Hardwick et al., 1992), we have also investigated the role of this receptor in *ras* transformation. We show here that disruption of RHAMM function by antisense RNA expression or by a dominant negative mutant of RHAMM profoundly reduces the transforming properties of the *ras* oncogene. We also link the ability of the dominant negative RHAMM mutation to ablate *ras* transformation to an effect on signaling via the focal adhesion kinase (FAK), pp125^{FAK}, within focal adhesions.

Results

Overexpression of RHAMM in Fibroblasts Induces Transformation

Since it had been previously shown that RHAMM expression was elevated in *ras*-transformed cells (Turley et al., 1991; Hardwick et al., 1992; Samuel et al., 1993), the contribution of RHAMM to the transformation process was investigated by its overexpression in nonsenescing fibroblasts. 10T½ fibroblasts were transfected with either a genomic RHAMM clone, λ4 (Hardwick et al., 1992; Entwistle et al., 1995), or a RHAMM cDNA encoding an isoform common to *ras*-transformed cells (RHAMM 1v4, Zhang et al., submitted). Both transfections were chemically selected, and cell lines were cloned. Five clones that overexpressed RHAMM, as determined by Western blot analysis of cell lysates (Table 1) and Northern blot analysis of RHAMM RNA (data not shown), were selected from each transfection. These selected clones were further characterized, and their properties are summarized in Table 1.

*The first two authors contributed equally to this work.

Table 1. Characteristics of RHAMM-Transfected 10T½ Clones

Cell Line	Densitometry of RHAMM Western Blot Analysis	FACS[a] Mean Fluorescent Intensity	Rate of Motility (μM/hr ± SEM) Control	Rate of Motility (μM/hr ± SEM) Anti-RHAMM Antibody	Foci per Dish	Nuclear Overlap Rate	Subcutaneous Tumors in Mice	Spontaneous Metastases
10T½ fibroblast	0.31	2.4	10.0 ± 0.84	8.6 ± 1.2	13 ± 4	0.01	0 of 4	0 of 8
C3 fibrosarcoma	1.35	85.0	35.1 ± 2.2	10.2 ± 1.4	77 ± 9	0.45	4 of 4	ND
Genomic RHAMM transfectants								
Vector only	0.54	2.5	10.6 ± 0.9	9.9 ± 0.4	12 ± 3	0.02	0 of 4	0 of 8
λ4-2-10T½	1.29	82.5	36.6 ± 4.4	ND	ND	0.36	ND	ND
λ4-6-10T½	2.20	43.0	31.8 ± 2.0	ND	ND	0.25	ND	ND
λ4-10-10T½	1.08	74.8	25.6 ± 1.7	10.9 ± 1.7	150 ± 7	0.49	4 of 4	ND
λ4-12-10T½	2.77	116.0	36.1 ± 2.2	11.7 ± 0.5	249 ± 16	0.42	4 of 4	4 of 8[b]
RHAMM cDNA transfectants								
Vector only	0.35	3.9	9.8 ± 0.5	9.8	11 ± 4	0.01	0 of 4	ND
cDNA 5-10T½	2.65	74.8	24.5 ± 2.3	10.1 ± 2.1	240 ± 10	0.41	4 of 4	ND
cDNA-3T3	ND	ND	ND	ND	250 ± 10	ND	4 of 4	ND
MR-10T½-4	1.56	81.3	11.1 ± 0.6	9.3 ± 1.2	0	0.01	0 of 4	ND

10T½ cells were transfected with genomic RHAMM (λ4) for clones 2, 6, 10, and 12, RHAMM cDNA (RHAMM 1v4; Entwistle et al., 1995) for clone cDNA 5-10T½ or RHAMM cDNA mutated in its HA-binding domains for clone MR-10T½-4. NIH 3T3 cells were transfected with RHAMM cDNA (RHAMM 1v4) for clone cDNA-3T3. Characteristics were determined as outlined in Experimental Procedures. Motility rate was obtained by tracking 100 cells. ND, not determined.

[a] Corrected for background fluorescence in the presence of normal IgG.

[b] Mean of five colonies per lung.

Cells transfected with the RHAMM gene overexpressed a 73 kDa protein consistent with the predicted size of RHAMM (data not shown; Entwistle et al., 1995). The same cells displayed an increase in a 4.2 kb message, the size of the major RHAMM mRNA transcript (data not shown; Hardwick et al., 1992). The presence of the transfected RHAMM gene in all clones was confirmed by polymerase chain reaction (PCR) detection of plasmid arms (data not shown). The selected clones overexpressed products of the RHAMM gene at the cell surface as determined by fluorescence-activated cell sorter (FACS) analysis (Table 1). Transfected cells appeared morphologically transformed (in that they were rounded), showed no evidence of contact inhibition, and possessed few focal adhesions (data not shown). Moreover, they exhibited a high nuclear overlap index comparable with that of *ras*-transformed cells (Table 1) and formed foci in monolayer culture, unlike the vector controls or the 10T½ parent cell line (Table 1). Furthermore, transfected cells reached culture confluence at a 3-fold to 4-fold higher cell number relative to vector control or parent line controls (data not shown). The rate of random locomotion of the transfected cells was 2-fold to 3-fold higher than control cell lines, a rate comparable with the *ras*-transformed C3 cell line (Table 1). This high motility was maintained at subconfluence and was blocked by anti-RHAMM antibodies (Table 1). The rate of growth of RHAMM-transfected cell lines was less than that of *ras*-transformed C3 cells and was, in fact, identical to that of the control cells until confluence halted growth of the latter. Nevertheless, RHAMM-transfected cells grew in an anchorage-independent fashion in soft agar (data not shown). Similar results on cell behavior were obtained after transfection of the RHAMM 1v4 cDNA in a pHβ APr-1-neo vector into 10T½ or 3T3 fibroblasts (Table 1). Transfection of RHAMM 1v4 cDNA containing mutated HA-binding domains (Figure 1) had no effect on morphology, contact inhibition, or motility (Table 1).

To determine whether cells transfected with the RHAMM λ4 gene were tumorigenic, we subcutaneously injected 1×10^6 to 5×10^6 cells into the right hind leg of syngeneic mice. Fibrosarcomas formed within 3 weeks; no tumors formed in mice injected with vector-transfected or 10T½ parental control cells (Table 1). Tumors derived from the transfected cells were identical histologically to those formed by *ras*-transformed cells and expressed high levels of RHAMM, as seen immunohistochemically. Further, in approximately 50% of animals bearing subcutaneous tumors, tumors spontaneously metastasized to the lung to form a mean of five nodules per lung (Table 1). The occurrence of tumor cells within these nodules was confirmed by histology. Cells injected into mice via the tail vein invaded lung tissue and formed metastatic nodules (Table 1). Cells transfected with RHAMM 1v4 cDNA were also tumorigenic and metastatic, but cells expressing the mutated RHAMM 1v4, lacking HA-binding domains, were not (Table 1).

These results were repeated with NIH 3T3 fibroblast cell line. We subcutaneously inoculated 5×10^6 transfected cells into syngeneic mice, and the presence of tumors was observed by 3 weeks (Table 1).

Reversion of H-*ras* Transformation with a Dominant Suppressor Mutant of RHAMM

The importance of RHAMM for maintenance of the transformed phenotype of H-*ras*–transformed fibrosarcomas was examined by blockade of RHAMM function with a

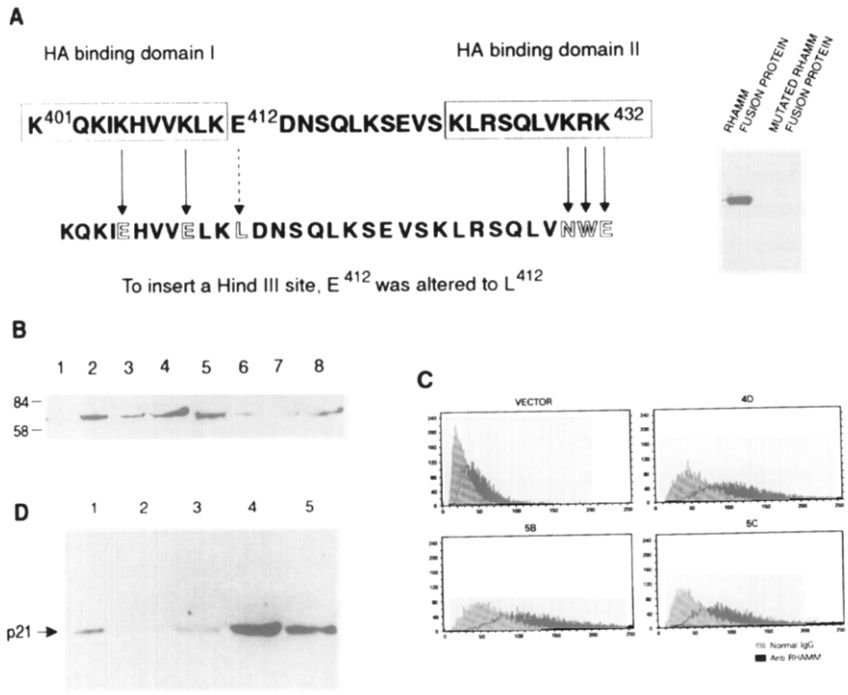

Figure 1. Reversion of H-*ras*–Transformed C3 Fibrosarcomas by Expression of RHAMM Mutated in Its HA-Binding Domain

(A) Strategy for mutating the HA-binding domains (boxed) of RHAMM. Lysines (K) and arginines (R) were altered as indicated, and this alteration has been shown to destroy the HA-binding properties of the RHAMM protein (Yang et al., 1994). RHAMM fusion protein was prepared from the intact cDNA (designated RHAMM fusion protein), electrophoresed, and assayed for biotinylated HA binding in a transblot assay. Fusion protein was produced from the RHAMM cDNA, which was mutated as described in Experimental Procedures. Mutated RHAMM fusion protein did not bind HA.

(B) C3 cell lysates were prepared from cells that were transfected with vector control (lanes 1 and 5) or mutated RHAMM cDNA (lanes 2–4 and 6–8, which represent clones MR-C3-4D, MR-C3-5B, and MR-C3-5C) and were electrophoresed and analysed for RHAMM using a Western transblot analysis (lanes 1–4). The blot was then stripped and reprobed with biotinylated HA (lanes 5–8). RHAMM was overexpressed in the transfected cell lines, but RHAMM from these cells bound less HA than controls, consistent with a dominant negative action by the mutated protein.

(C) Total RHAMM expression on the cell membrane assessed by FACS analysis revealed major increases in MR-C3 clones relative to the vector control.

(D) Cell lysates were obtained from C3 vector controls (lane 1), 10T½ fibroblasts (lane 2), and the three MR-C3 clones, MR-C3-4D, MR-C3-5B, and MR-C3-5C (lanes 3–5, respectively) and electrophoresed; $p21^{ras}$ was then visualized in a Western transblot analysis using a pan-specific anti-Ras antibody. All of the MR-C3–transfected clones expressed high levels of $p21^{ras}$, comparable with C3 (lane 1).

RHAMM cDNA mutated at its HA-binding domains (Figure 1). Similar suppressor mutations have been previously prepared by mutating the kinase domain (Evans et al., 1993) or by deleting the cytoplasmic domains of other receptors (Kashles et al., 1991). The present approach to functional ablation was taken because RHAMM is secreted, is localized at the cell surface, and forms homodimers (Hardwick et al., 1992; Klewes et al., 1993). Furthermore, mutation of the HA-binding domains in RHAMM destroys its ability to transform fibroblasts morphologically (Table 1). Collectively, these conditions have been found to be sufficient to construct suppressor mutations of such growth-factor receptors as TGFβ1 (Brand et al., 1993). The details of the amino acid substitutions in the HA-binding domains of RHAMM are outlined in Figure 1A. Loss of HA binding was confirmed using the mutated RHAMM fusion protein in a ligand blotting assay, the specificity of which has previously been demonstrated (Figure 1A; Hoare et al., 1993). *ras*-transformed 10T½ fibroblasts (termed C3) were transfected with the mutated RHAMM and chemically selected in hygromycin. Over 20 clones were selected, 25% of which displayed a flattened cell shape that was morphologically similar to 10T½ fibroblasts not transformed by *ras* (Figure 2C). Three clones containing the mutated RHAMM protein were selected for further analysis, and all three were found to overexpress RHAMM by 2-fold to 3-fold, as determined by Western blot analysis (for examples see Figure 1B, lanes 2–4). Increased cell-surface expression of RHAMM was detected by FACS analysis (see Figure 1D) using antibody A268 (Hardwick et al., 1992), which specifically recognizes a peptide encoded in the RHAMM cDNA (amino acids 268–289) that is 5′ to the mutated region of the protein (see Figure 1C). Despite their flattened morphology, all clones overexpressing mutant RHAMM exhibited levels of $p21^{ras}$ protein that were comparable with or higher than those seen in the H-*ras*–transformed C3 fibrosarcoma cells transfected with vector only (see Figure 1C).

Despite the expression of high levels of activated *ras*, clones expressing the suppressor mutant of RHAMM (MR-C3-4D, MR-C3-5B, and MR-C3-5C) more closely resembled the nontransformed 10T½ cells in their growth characteristics, locomotion rates, and tumorigenic capabilities. Mutated RHAMM clones were contact inhibited and displayed a low nuclear overlap ratio, comparable with that of the nontransformed 10T½ cell line (Figures 2A–2C). They had a lower saturation density than *ras*-transformed vector control cells (Figure 2D) and showed suppressed rates of locomotion in comparison with transformed parental C3 fibrosarcoma cells (Table 2). In contrast with vector-transfected controls, the cells expressing the dominant suppressor RHAMM failed to form foci in monolayer cultures (Figure 2E) and did not form colonies in soft agar (Table 2). When injected subcutaneously into syngeneic mice, no tumors were detected after 6 months of observation (Figure 2F), while vector controls and the *ras*–10T½ parent cell line formed large tumors within 3 weeks (Figure 2F). In addition, the clones expressing mutated RHAMM did not develop tumors in the lung colonization assay for metastasis (Figure 2G).

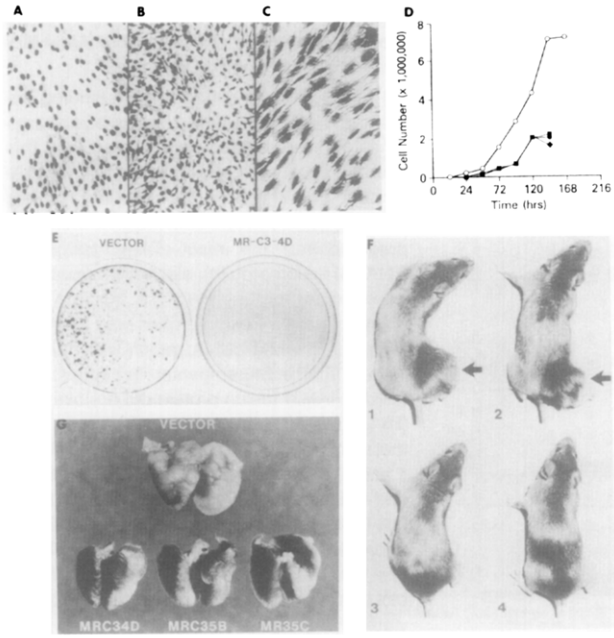

Figure 2. Morphological and Growth Properties of Dominant Negative Mutant Transfected C3 Cells

(A–C) Cell morphology of transfected cell lines including 10T½ parent line (A), vector-transfected C3 cells (B), and MR-C3–transfected cells (C). The MR-C3 cells resemble the nontransformed 10T½ line, appearing flattened and contact inhibited in contrast with the vector-transfected *ras*-transformed parent C3 line.

(D) Growth curve of vector control–transfected C3 cells (open circles) and MR-C3-3D (closed diamond), MR-C3-5B (closed square), and MR-C3-5C (closed circle) clones. We plated 5 × 10^4 cells, and the number of cells was counted each day with a Coulter counter. The vector control–transfected cells grow more rapidly than the mutant RHAMM–transfected *ras*-transformed cells and reach a much higher saturation density.

(E) A focus-forming assay was performed as described in Experimental Procedures using vector control–transfected C3 cells and MR-C3-4D clone. The vector controls formed multiple foci in dense culture, while the cells transfected with mutated RHAMM did not form foci.

(F) Mice injected with either C3 parent line (1) or vector control (2) formed large fibrosarcomas (arrows) by 3 weeks after injection. Mice injected with MR-C3-4D (3) or MR-C3-5C (4) clones did not form tumors after 6 months of observation.

(G) The vector control C3 control injected into the tail vein of mice formed multiple lung colonies in the mouse (top). None of the three MR-C3 clones (MR-C3-4D, MR-C3-5B, and MR-C3-5C) formed detectable colonies (bottom).

Expression of Dominant Suppressor RHAMM Ablates Signal Transduction to Focal Adhesions

We have previously shown that in *ras*-transformed fibroblasts RHAMM signals cell locomotion via a transient tyrosine phosphorylation pathway that targets focal adhesions (Hall et al., 1994). Stimulation of these cells results in two rapid and transient events: tyrosine phosphorylation of several protein bands and the formation of focal adhesions. Net dephosphorylation and focal adhesion turnover rapidly follow concomitant with elevated cell motility. Since expression of the dominant suppressor RHAMM inhibits cell locomotion, among other transformation-dependent processes (Table 2), we examined the effect of this protein on signal transduction and focal adhesions. Vector-transfected C3 cells responded to HA stimulation as previously reported (Hall et al., 1994), with a transient increase in the phosphorylation of several protein bands (p185, p125, p115, and p85), followed by net dephosphorylation (Figure 3A). In particular, $pp125^{FAK}$ has been identified as a substrate in this pathway (Hall et al., 1994). Transient tyrosine phosphorylation of this substrate, followed by dephosphorylation, coincidental with focal adhesion turnover, is observed in vector control cells (Figure 3B). Tyrosine phosphorylation of FAK and other protein bands in the dominant suppressor–expressing cells (MR-C3-4D) remained constant over the stimulation time course (Figures 3A and 3B). Thus, *ras*-transformed fibroblasts expressing the dominant suppressor RHAMM cannot utilize the signal transduction pathway that involves changes in FAK phosphorylation and that is required for transformation by *ras*.

Cells possessing stable focal adhesions move more slowly and are less tumorigenic (see Discussion). *ras*-transformed fibroblasts normally have very few focal adhesions, but form temporary focal adhesions at the cell edge after HA stimulation (vector control, Figure 3Ca). On the contrary, the cells expressing the HA binding–deficient RHAMM have numerous focal adhesions throughout the cell in the presence or absence of HA (Figure 3Cb), thus resembling nontransformed 10T½ fibroblasts. Similarly, tyrosine phosphorylation levels in these cells are higher and largely occur in the focal adhesions (Figure 3Cd). The HA-stimulated vector control cells exhibit rapid onset of increased phosphotyrosine staining only at the lamellae edges and only at 1 min after stimulation with HA, while

Table 2. Suppression of Transformation by Expression of RHAMM Mutated in Its HA-Binding Domain

Cell Line	Growth in Soft Agar (Colonies ± SEM)	Nuclear Overlap Ratio	Foci per Dish	Rate of Motility (μM/hr ± SEM)
10T½	0	0.01	0	9.5 ± 1.3
C3 vector control	77 ± 9	0.47	>60	27.5 ± 1.2
MR-C3-4D	0	0.005	0	3.5 ± 0.8
MR-C3-5B	1 ± 1	0.004	0	1.8 ± 0.5
MR-C3-5C	0	0.005	0	2.0 ± 0.6

The H-*ras*–transformed C3 fibrosarcoma was transfected either with vector control (C3 vector control) or with RHAMM (Entwistle et al., 1995) mutated in its HA-binding domain (MR-C3-4D, MR-C3-5B, MR-C3-5C), while 10T½ is the nontransformed parental line of the C3.

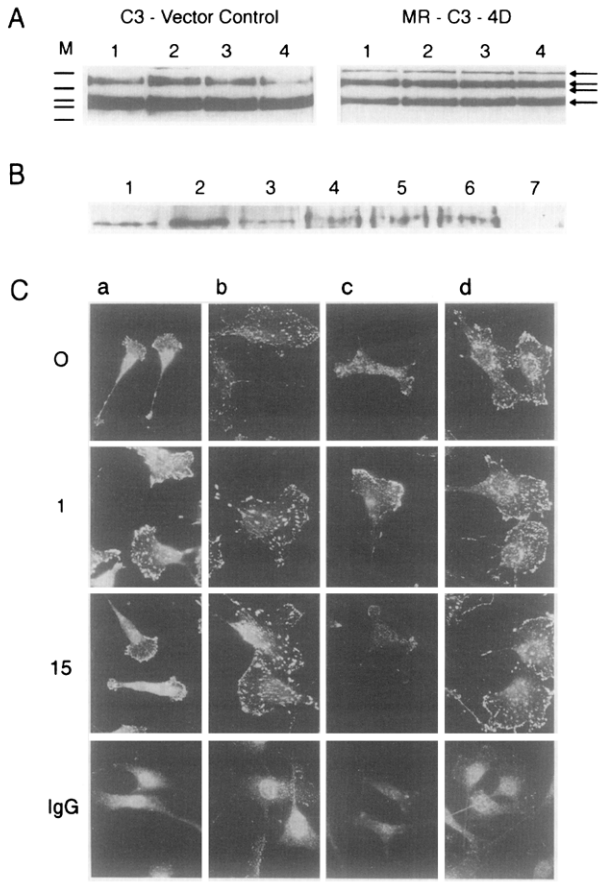

Figure 3. Overexpression of Dominant Suppressor RHAMM Prevents Tyrosine Phosphorylation, Focal Adhesion Kinase Dephosphorylation, and Focal Adhesion Turnover in *ras*-Transformed Fibroblasts

(A) Cultures (24 hr) of vector control C3 fibroblasts (left) and MR-C3-4D (right) were stimulated with HA (10 ng/ml) for 0 min (lane 1), 1 min (lane 2), 5 min (lane 3), or 15 min (lane 4) prior to cell lysis. Equal protein concentrations from each sample were run on SDS–polyacrylamide gels, transferred to nitrocellulose, and subjected to anti-phosphotyrosine immunoblot analysis. Vector control cells displayed a rapid and transient increase in the tyrosine phosphorylation of p185, p125, p115, and p85 (arrows), followed by a decrease in the phosphorylation of these protein bands, as did the *ras*–10T½ C3 fibroblasts (data not shown). The level of tyrosine phosphorylation in the MR-C3-4D cells did not change with HA treatment. Similar results were obtained with the clone MR-C3-5C (data not shown). The molecular markers (M) indicate 190, 125, 88, and 65 kDa.

(B) Cell cultures of vector control C3 fibroblasts and mutated RHAMM–overexpressers MR-C3-4D were stimulated as described above for 1 min (lanes 2 and 5) or 15 min (lanes 3 and 6) with HA or with buffer alone (lanes 1 and 4) and then were lysed in RIPA buffer. Immunoprecipitation was performed with anti-FAK (lanes 1–6) or mouse IgG control (lane 7), followed by SDS–polyacrylamide gel electrophoresis and anti-phosphotyrosine immunoblot analysis. Vector control fibroblasts (lanes 1–3) exhibit an increase followed by a decrease in FAK phosphorylation. The MR-C3-4D cells (lanes 4–6) show no change in FAK phosphorylation with HA treatment.

(C) Immunofluorescent localization of vinculin and phosphotyrosine in vector control C3 and MR-C3-4D fibroblasts before and after HA treatment. Fibroblasts were incubated in the absence (0) or presence of 10 ng/ml HA for 1 min (1 and IgG) or 15 min (15) before fixation and staining with anti-vinculin (a and b) and anti-phosphotyrosine (c and d). Mouse IgG control panels are shown (bottom row). Vector control cells (a and c) exposed to HA for 1 min show an increase in both focal adhesions (anti-vinculin) and anti-phosphotyrosine staining, which then decreases by 15 min of treatment. MR-C3-4D (b and d) and MR-C3-5C (data not shown) display focal adhesions and phosphotyrosine staining that do not change with treatment.

the MR-C3-4D cells do not respond to HA, but maintain high levels of plaque-like phosphotyrosine staining in the cell body and at the lamellae edges (Figure 3Cc and 3Cd).

Antisense RHAMM Confers Resistance to Transformation by Mutant H-*ras*

To determine whether fibroblasts with suppressed RHAMM expression could be transformed with *ras*, we transfected 10T½ cells with RHAMM cDNA in an antisense orientation. Two G418 resistant clones (termed OR1 and OR2) that expressed 10%–50% of the detectable RHAMM protein levels seen in vector controls were selected from over 60 clones with varying reductions of RHAMM expression (X. Y. et al., unpublished data). The two clones expressing low levels of RHAMM protein were identical in their properties. The presence of RHAMM antisense and the reduction or lack of RHAMM message was demonstrated by reverse transcription–PCR (RT–PCR) and confirmed by Southern blot hybridization (X. Y. et al., unpublished data). The two transfected cell lines, the vector control, and the parent 10T½ cells were then grown to confluence and transfected with an activated H-*ras*. The vector control and the parental line formed multiple large and small foci after 3 weeks in culture (Figures 4A–4B), whereas cultures containing the OR1 and OR2 constructs formed no such foci (Figures

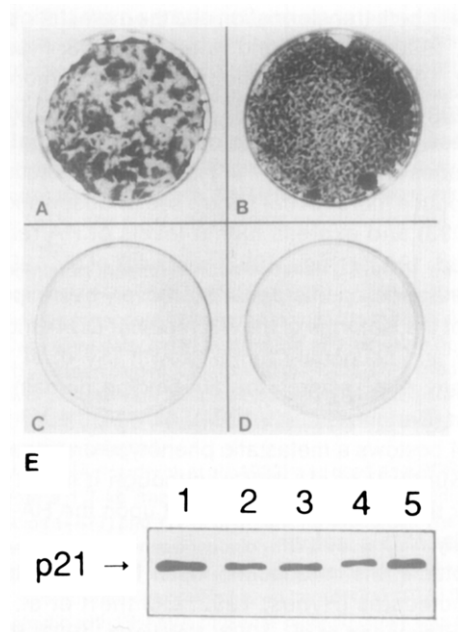

Figure 4. Inhibition of Transformation by Mutant H-*ras* in Fibroblasts Expressing Antisense RHAMM Clones OR1 and OR2

10T½ parent cells transfected with *ras* (A), vector control 10T½ cells transfected with *ras* (B), OR1 clone transfected with *ras* (C), and OR2 clone transfected with *ras* (D). *ras* vector exhibited multiple large foci formed in controls, but clones transfected with RHAMM antisense did not form foci. (E) Ras protein is expressed in *ras*-transfected OR1 and OR2 fibroblasts. All cells transfected with *ras* (lane 1, *ras*-transformed C3 cells; lane 2, antisense vector, only 10T½ clone 1; lane 3, antisense vector, only 10T½ clone 2; lane 4, OR1 cells; lane 5, OR2 cells) expressed $p21^{ras}$ protein, as detected in a Western blot assay with a pan-*ras* antibody. Levels of expression (lanes 2–5) are approximately equivalent and are higher than normally expressed in parental 10T½ cells (see Figure 2D).

4C–4D). Furthermore, these clones, unlike *ras*-transformed controls, retained a flattened morphology. All *ras*-transfected cultures expressed $p21^{ras}$ protein (Figure 4E) at levels similar to those of the *ras*-transformed cell line C3 (compare Figure 4E with Figure 1C).

Discussion

We demonstrate here that the HA receptor RHAMM, a GPI-linked plasma membrane protein (L. Klewes et al., unpublished data), is not only transforming, but that its expression is sufficient to generate a metastatic fibrosarcoma. In addition, RHAMM also appears to be necessary for initiating and maintaining transformation induced by other oncogenes, such as *ras*. Since *ras*-transformed cells expressing nonfunctional RHAMM are unable to signal and turn over focal adhesions, these results also imply a direct role for RHAMM in signaling within these cytoskeletal structures in the transformation process downstream of *ras*.

The transforming capability of RHAMM and the inability of RHAMM mutated in its HA-binding domains to transform cells demonstrate a causal role for HA in the transformation process. The observation that mutation of RHAMM in its HA-binding domains ablates *ras* transformation provides further evidence connecting HA to transformation. HA, a ubiquitous glycosaminoglycan, has previously been linked with both transformation and the metastatic process (Turley, 1992; Knudson and Knudson, 1993; Fraser and Laurent, 1993), since it is often enriched in tumor-associated stroma (Turley and Tretiak, 1984) and its presence facilitates melanoma invasion across chorioallantoic membranes (Turley et al., 1987). Highly metastatic tumor cells produce more HA (for review see Knudson and Knudson, 1993) and express higher levels of HA receptors (Günthert, 1993; Hynes, 1992; Hardwick et al., 1992) than less metastatic counterparts. Moreover, overexpression of one of the isoforms of the HA receptor CD44 increases primary and secondary tumor growth (Sy et al., 1991), a property that requires the HA-binding domain of this receptor (Bartolazzi et al., 1994). As well, the V6 isoform of CD44 bestows a metastatic phenotype on transformed cells (Günthert et al., 1991), although it is not known whether this property is dependent upon the HA-binding capability of this isoform.

As noted in the introduction, other ECM receptors and ECM molecules (Hynes, 1992; Günthert et al., 1991; Stetler-Stevenson et al., 1993; Schwartz, 1993; Behrend et al., 1994) have also been linked to the regulation of the invasive properties of cells or to the partial modification of the transformation process itself. It is important to note, however, that none of these molecules has been demonstrated to be transforming by itself, implying that RHAMM has a unique role in orchestrating events that are essential for transformation to occur. These events include the ability of RHAMM to signal, via focal adhesions, alterations in the cytoskeleton and elevated cell locomotion.

Focal adhesions are sites of ECM receptor–cytoskeletal interactions, where second-messenger signaling commonly occurs in response to the ECM and some growth factor receptors. These structures, also described as signal transduction units (Lo and Chen, 1994; Zachary and Rozengurt, 1992), are believed to be critical for the regulation of growth and cell motility (Woods and Couchman, 1988; Burridge et al., 1988). They have previously been linked to transformation, in that very few focal adhesions are present in tumor cells (Burridge et al., 1988) and focal adhesion assembly promoted by overexpression of the focal adhesion components, $\alpha5\beta1$ integrin, tensin, or vinculin, causes partial reversal of transformation (Giancotti and Ruoslahti, 1990; Varner et al., 1992; Lo and Chen, 1994). Conversely, antisense ablated expression of the focal adhesion protein vinculin promotes transformation-dependent properties (Rodriguez-Fernández et al., 1993); as well, the selective targeting of truncated v-*src* to focal adhesions, but not to the nucleus or to the cytoplasm, is sufficient for transformation by this oncogene (Leibl and Martin, 1992). We have previously noted that in *ras*-transformed fibroblasts, unlike their parental counterparts, HA regulates cell motility via RHAMM by signaling transient protein-tyrosine phosphorylation within focal adhesions (Hall et al., 1994). In this signaling pathway, FAK is transiently phosphorylated, followed by net dephosphorylation and focal adhesion turnover leading to the initiation of cell locomotion (Hall et al., 1994). Cells overexpressing RHAMM resemble *ras*-transformed fibroblasts and have elevated cell locomotion and focal adhesion loss, as well as tumorigenic and metastatic potential. Conversely, expression of a dominant suppressor mutant of RHAMM reverts transformation induced by *ras* and stabilizes focal adhesions (X. Y. et al., unpublished data). This HA receptor targets focal adhesions and likely acts downstream of *ras* or via a parallel pathway that converges at the level of *ras*.

FAK has been implicated in several signaling pathways that involve ECM receptors, as well as in transformation (Schaller et al., 1992; Calalb et al., 1994). The stimulation of activation by growth factors, neuropeptides, and the ECM is associated with cell attachment, focal adhesion assembly, and stress fiber formation (Schaller and Parsons, 1994; Zachary and Rozengurt, 1992). Cell adhesion via integrins can stimulate the formation of signaling complexes containing FAK, c-*src*, Grb-2, and Sos (Schlaepfer et al., 1994), thus providing a mechanism for the regulation of the *ras*/MAP kinase signaling cascade downstream of FAK phosphorylation. On the contrary, transient FAK phosphorylation, followed by net FAK dephosphorylation, has been associated with elevated cell migration (Hall et al., 1994; Matsumoto et al., 1994) and, hence, may represent the mechanism by which *ras* and RHAMM regulate elevated cell motility. We show here that a dominant suppressor mutation of RHAMM that ablates *ras* transformation collectively prevents HA binding, HA-triggered FAK signaling, focal adhesion turnover, and cell motility. Thus, while integrin and growth factor–regulated FAK phosphorylation would appear to be upstream of *ras* signaling, our results indicate that FAK dephosphorylation, regulated by RHAMM, acts downstream of mutant *ras* and is an event

that is required for transformation by this oncogene. While our results specifically suggest that the constitutive ability to turn over focal adhesions is a requirement for *ras* transformation, this event by itself is unlikely to be sufficient for transformation to occur. Hence, the overexpression of either of the ECM components, thrombospondin or tenascin, reduces focal adhesion assembly (Borsi et al., 1992; Murphy-Ullrich and Hook, 1989), but both are only partially transforming, merely enhancing serum- and anchorage-independent growth of immortalized cell lines (Castle et al., 1993; Murphy-Ullrich et al., 1991; Wehrle-Haller and Chiquet, 1993). Also, loss of focal adhesions induced by the overexpression of a truncated rasGAP has little effect on growth potential (McGlade et al., 1993). The regulation of focal adhesion turnover, probably effected by dephosphorylation of FAK, is likely required for transformation to occur, but is unlikely to account for the tumorigenic/metastatic properties. Thus, overexpression of RHAMM must result in transformation by altering additional cell characteristics.

Signaling via tyrosine phosphorylation has previously been identified as an event that can lead to transformation, and since RHAMM transiently activates protein phosphorylation, such signaling may ultimately lead not only to focal adhesion turnover, but also to selective expression of genes that act collectively through *ras* to transform the cell. Previous reports link signal transduction pathways mediated by other ECM receptors (Damsky and Werb, 1992; Hynes, 1992; Juliano and Haskill, 1993; Schwartz, 1993) to changes in gene expression (Jones et al., 1993). Mammary epithelial cells produce tissue-specific proteins in response to basement membranes (Howlett and Bissell, 1993), while laminin, fibronectin, and other ECM components regulate stromelysin, collagenase (Werb et al., 1989; Shapiro et al., 1993; Saarialho-Kere et al., 1993), and other genes (Jones et al., 1993). HA has also previously been reported to regulate the expression of several cytokine genes, in part via CD44 (Noble et al., 1993; Chong et al., 1992). It is likely therefore that other genes are also regulated by RHAMM.

In summary, we have demonstrated that overexpression of RHAMM is transforming and that ablation of RHAMM expression or its function prevents *ras* transformation. We also provide direct evidence of a role for signaling within focal adhesions for maintaining *ras* transformation.

Experimental Procedures

Cell Culture and Cell Lines

The previously established murine fibroblast cell lines 10T½, NIH 3T3, and the H-*ras*–10T½ CIRAS-3 (C3; Egan et al., 1987) were utilized for the various transfection and tumorigenic studies. The cells were maintained at 37°C in 5% CO_2 in DMEM growth media (GIBCO BRL) supplemented with 10% fetal calf serum (Invitrogen). Cells were subcultured using trypsin and EDTA (0.25% Difco bactotrypsin, 2 mM EDTA) prior to reaching confluence. To determine culture density, we added 5 × 10^4 cells to each of 24 wells in 1 ml of DMEM supplemented with 10% FCS and 0.6 mg/ml geneticin. Medium was changed every 3 days, and at each timepoint cells were released from the substratum with 0.25% trypsin and counted with a Coulter counter.

Preparation of DNA Constructs

The full-length RHAMM gene was isolated from a 3T3 cell genomic library and is described elsewhere (Entwistle et al., 1995). The genomic RHAMM clone λ4 was harbored in EMBL3 phage arms for transfection. RHAMM cDNAs, mutated cDNAs, and antisense cDNAs (Hardwick et al., 1992; Entwistle et al., 1995) were cloned into the pHβ APr-1–neo expression vector (Gunning et al., 1987). The cDNAs mutated in their HA-binding domains have been described previously (Yang et al., 1994). In brief, mutagenesis of specific basic amino acids in both of the HA-binding domains of RHAMM was accomplished in two steps. First, site-directed mutations were confined to basic amino acids Lys-405 and Lys-409. Next, the basic amino acids 430 and 432 were mutated using the RHAMM cDNA generated in the first step. The mutations abolish HA binding of the resulting protein (Figure 1; Yang et al., 1994). The RHAMM antisense cDNA was produced by PCR of the entire coding region (amino acids 1–477; Hardwick et al., 1992) and 172 nt of the 3′ flanking sequence. The fragment cloned into the expression vector in the antisense orientation was sequenced for confirmation.

Transfection with Genomic RHAMM in RHAMM cDNAs

The RHAMM λ4 clone in EMBL3 phage arms was cotransfected with PSV_2 plasmid into 10T½ fibroblasts using calcium phosphate. RHAMM-transfected cells were selectively grown in growth media containing 0.6 mg/ml G418 for 3 weeks, colonies were cloned by selective trypsinization, and 15 clones were isolated. Four clones (λ4-2–10T½, λ4-6–10T½, λ4-10–10T½, and λ4-12–10T½) that exhibited stable integration of the RHAMM gene by Southern blot analysis and overexpression of the RHAMM protein by immunoblot analysis were selected for further study.

10T½ and NIH 3T3 cell lines were transfected with either the RHAMM 1v4 cDNA construct (Entwistle et al., 1995; S. Z. et al., unpublished data) in the pHβ Apr-1–neo expression vector (Gunning et al., 1987) or the RHAMM 1v4 cDNA mutated construct as described above. To produce stably transfected cell lines, we transfected fibroblasts using lipofectin (GIBCO BRL) according to the instructions of the manufacturer, and cells were selected in G418. Clones were then selected as above and tested for overexpression using Western blot analysis (S. Z. et al., unpublished data). Based on their overexpression and representative morphology, the following clones were used in this study: vector-transfected cells, RHAMM 1v4–overexpressing clones (cDNA 5–10T½ and cDNA–3T3), and a mutated RHAMM 1v4 clone (MR–10T½-4).

For dominant negative transfections, C3 cells were stably transfected with the mutated RHAMM cDNAs as described above, except that the hygromycin gene was included in the pHβ APr-1–neo vector. Cells were selected in hygromycin and geneticin (to maintain *ras* insert) and then cloned. Clones that exhibited a flattened morphology (45% of clones) were selected and then analyzed for overexpression of RHAMM using a Western transblot assay. Three high expressing clones were selected.

RHAMM cDNA (Hardwick et al., 1992) was used as a PCR template to generate a 1.7 kb fragment containing the entire coding region (amino acids 1–477) and 172 nt of 3′ flanking sequence. The fragment was cloned in an antisense orientation into the pHβ Apr-1–neo expression vector (Gunning et al., 1987) and sequenced for confirmation. To produce stably transfected cell lines, we transfected 10T½ fibroblasts using lipofectin with RHAMM antisense plasmid constructs according to the instructions of the manufacturer (GIBCO BRL). In brief, 1 × 10^5 to 2 × 10^5 of the 10T½ cells were seeded into 60 mm tissue culture dishes and cultured in growth medium containing DMEM and 10% fetal bovine serum. After reaching 50%–70% confluence, cells were transfected with 10–20 μg of RHAMM plasmid, selected in G418, and then cloned. Low production of RHAMM was detected by Western blot analysis and RT-PCR.

Cell Lysis and Immunoblot Analysis

C3 cell cultures were exposed to HA (10 ng/ml; Hall et al., 1994) or control treatments for various time periods at 37°C and then placed on ice. Culture medium was removed, the plates were rinsed with cold PBS (2.7 mM KCl, 1.1 mM KH_2PO_4, 138 mM NaCl, 8.1 mM Na_2HPO_4 [pH 7.4]) containing 250 μM sodium orthovanadate, and the cells were

lysed with ice cold RIPA lysis buffer (25 mM Tris [pH 7.2], 0.1% SDS, 1% Triton X-100, 1% sodium dexoycholate, 0.15 M NaCl, 1 mM EDTA) containing 10 μg/ml leupeptin, 10 μg/ml aprotinin, 1 mM PMSF, and 1 mM sodium orthovanadate (all chemicals from Sigma). Lysates were scraped into microcentrifuge tubes and after 10 min on ice were centrifuged at 13,000 rpm for 15 min at 4°C (Heraus Biofuge 13, Baxter Diagnostics). Protein concentrations of the supernatants and BSA standards were determined using the DC protein assay (Bio-Rad), and duplicate samples containing 20 μg of protein each along with prestained molecular weight markers (Sigma) were separated by SDS–PAGE (12% gel). The proteins on the gels were either electrophoretically transferred to nitrocellulose membranes (Bio-Rad) or stained with Coomassie blue to check for equal loading. Additional protein-binding sites on the nitrocellulose membranes were blocked with 5% defatted milk in TBS (50 mM Tris–HCl [pH 7.4], 200 mM NaCl), and then the membranes were incubated with anti-phosphotyrosine MAb 4G10 (1 μg/ml [Upstate Biotechnology] in 1% defatted milk in TBS) or anti-RHAMM antibody (1:200; Yang et al., 1994) for 2 hr at room temperature on a rotator (Nutator, Becton Dickinson). The membranes were washed four times in 0.05% Tween 20 in TBS before incubation with peroxidase-conjugated goat anti-mouse secondary antibody (1:5000 dilution in 1% milk and Tween 20 in TBS; Sigma) for 1 hr at room temperature. After washing, blots were developed using the ECL Western blotting detection system (Amersham) according to the instructions of the manufacturer. To establish antibody specificity, we probed parallel blots with anti-phosphotyrosine that had been preincubated with 200 μM phosphotyrosine (Sigma) for 1 hr. Likewise, anti-RHAMM antibodies were preincubated with 200 μg of RHAMM fusion protein before incubation with membranes as above.

Immunoprecipitation

Cells were stimulated with HA and lysed as described above. Each sample (500 μg of protein) was incubated with anti-p125^{FAK} MAb (4 μg/ml monoclonal anti-FAK; Transduction Laboratories) and rabbit anti-mouse IgG (10 μg/ml; Sigma) for 1 hr at 4°C by mixing end-over-end. To cause precipitation, we added 100 μl of protein G–agarose (GIBCO BRL) to each tube, and the samples were mixed end-over-end for another 30 min at 4°C. The beads were pelleted by brief centrifugation at 13,000 rpm and washed three times with RIPA buffer. The proteins were released from the beads by boiling in Laemmli sample buffer and were then subjected to SDS–PAGE and anti-phosphotyrosine immunoblotting as described above. To assess whether equal quantities of FAK were immunoprecipitated from control and treated samples, the blots were stripped and reprobed with purified anti-FAK antibody 2A7 (10 μg/ml; a gift from J. T. Parsons).

Immunofluorescent Staining

Vector control *ras*–10T½, MR-C3-4D, and MR-C3-5C fibroblasts were grown on untreated or fibronectin-coated glass coverslips for 24 hr. The cells were exposed to HA (10 ng/ml), anti-RHAMM, or control treatment for 1 min and 15 min. At the appropriate time periods, the media was aspirated, and the cells were rinsed with PBS and then fixed with 3% paraformaldehyde (Sigma) in PBS for 10 min. Cells were washed three times for 10 min with wash solution (10% FCS in PBS containing 0.02% sodium azide), permeabilized with 0.2% Triton X-100 in PBS for 5 min, and washed three more times. The fixed cells were incubated at 37°C for 1 hr with anti-phosphotyrosine MAb 4G10 (5 μg/ml; Upstate Biotechnology), anti-vinculin MAb (1:50; Sigma), or appropriate IgG controls (Sigma) in wash solution. After being washed five times, coverslips were incubated with goat anti-mouse Cy3 (1:500; Jackson) for 3 hr. After washing, the coverslips were mounted onto glass slides using Fluoromount (BDH). Observations and photomicrographs were obtained with a Zeiss Axiovert 35× fluorescent microscope using epifluorescence.

Time-Lapse Cinemicrography

To monitor random locomotion, we plated 6×10^4 cells in 25 cm^2 tissue culture flasks 24 hr prior to measurement. Cell locomotion was quantified using an IM 35 inverted microscope (Zeiss), to which a video camera (Hamamatsu CCD) was attached. The cells were maintained at 37°C using a heated platform (TRZ 3700, Zeiss). Motility was measured using image analysis (Image 1, Universal Imaging). This program allows quantitation of nuclear displacement in a sequence of digitalized images.

Flow Cytometry

Cells were harvested using Hanks' balanced salt solution plus 20 mM HEPES, 0.05% sodium azide, and 2.0 mM EDTA for 5 min and were maintained at 4°C throughout the procedure. The cells were washed in the same solution except in the absence of EDTA and then incubated with anti-peptide (amino acids 268–288) antiserum (1:50 dilution; Hardwick et al., 1992) for 30 min. Following this, the cells were incubated with fluorescein-conjugated goat anti-rabbit antiserum (1:300 dilution; Sigma) for a further 30 min and were then fixed with 3% paraformaldehyde. The surface expression of RHAMM was studied using immunofluorescence flow cytometry. Normal IgG was used as a control at each timepoint analyzed.

HA Binding Assay

Proteins were electrophoresed on 10% SDS–polyacrylamide gel and transblotted onto a nitrocellulose membrane in a Tris–glycine buffer containing 25 mM Tris, 192 mM glycine, and 20% methanol (pH 8.3) at 80 V for 1 hr in a cold room. The membrane was blocked in 10 mM Tris–HCl (pH 8.0) containing 150 mM NaCl (TBS), 0.05% Tween 20 (TBST), and 5% skim milk powder (TBSTS) for 1 hr at room temperature and then incubated with biotinylated HA (Yang et al., 1994) and diluted in TBSTS (1:2000) overnight at 4°C. The membrane was washed with TBST extensively and then incubated with a streptavidin–peroxidase conjugate in TBSTS. Binding was visualized with chemiluminescence according to the instructions of the kit (ECL Kit, Amersham), which uses luminal and hydrogen peroxide to visualize the bound peroxidase.

Focus Formation

Cells were grown to 50% confluence and, in the case of RHAMM antisense-transfected clones, transfected with H-*ras* using lipofectin as described above or, in the case of RHAMM sense-transfected clones, buffer only. The cultures were then grown for 3–4 weeks in DMEM medium containing 10%–20% FBS. The medium was changed every 1–3 days for up to 4 weeks until foci formed. Foci were visualized with methylene blue staining and were counted per dish.

Growth in Soft Agar

We plated 5×10^3 cells per milliliter in bactoagar (1.25%) containing anti-MEM, 10% FBS for 7–10 days. Colonies of cells were counted per plate. The plating efficiency of each cell line was similar (75%).

Subcutaneous Tumor Formation and Tail Vein Assay

Cells were grown to confluence, washed with Hanks' solution and released from the substratum in Hanks' solution containing 2.5 mM EDTA. If cells did not release (i.e., 10T½ cells), they were scraped from the substratum with a rubber policeman. Exclusion of trypan blue indicated that >90% of cells treated in this manner were viable. C3 female mice were injected with 1×10^6 to 5×10^6 cells subcutaneously into the right hind leg and maintained for 3–6 weeks, when tumors routinely become apparent. Animals were euthanized, tumors were removed and weighed, and pieces were processed for histology using paraffin embedding techniques. Lungs were also excised and examined for tumor nodules, which, when present, were also processed for paraffin sections.

For experimental metastasis assays (Egan et al., 1987), 5×10^5 cells were injected into the tail vein. The mice were maintained for 6 weeks and then euthanized, lungs were removed, and the occurrence of tumor nodules was assessed by processing tissue for histology and examining tissue sections for tumor nodules.

Acknowledgments

This work was supported by National Cancer Institute of Canada (NCIC), Medical Research Council (MRC), and Hyal Pharmaceutical grants to E. A. T.; C. H. was supported by an MRC Studentship, B. Y. by a Manitoba Health Research Council Fellowship, and S. S. by an NCIC Fellowship. A. H. G. is a Terry Fox Scientist of the NCIC, and E. A. T. is a Children's Hospital Research Foundation Scholar.

Received September 15, 1994; revised May 12, 1995.

References

Alexander, C. M., and Werb, Z. (1992). Targeted disruption of the tissue inhibitor of metalloproteinases gene increases the invasive behaviour of primitive mesenchymal cells derived from embryonic stem cells *in vitro*. J. Cell Biol. *118*, 727–739.

Bartolazzi, A., Peach, R., Aruffo, A., and Stamenkovic, I. (1994). Interaction between CD44 and hyaluronate is directly implicated in the regulation of tumor development. J. Exp. Med. *180*, 53–66.

Behrend, E. J., Craig, A. M., Wilson, S. M., Denhardt, D. T., and Chambers, A. F. (1994). Reduced malignancy of *ras*-transformed NIH 3T3 cells expressing antisense osteopontin RNA. Cancer Res. *54*, 832–837.

Borsi, L., Carnemolla, B., Nicolo, G., Spina, B., Tanara, G., and Zardi, L. (1992). Expression of different tenascin isoforms in normal, hyperplastic and neoplastic human breast tissues. Int. J. Cancer *52*, 688–692.

Brand, T., MacLellan, W. R., and Schneider, M. D. (1993). A dominant-negative receptor for type β transforming growth factors created by deletion of the kinase domain. J. Biol. Chem. *268*, 11500–11503.

Burridge, K., Fath, K., Kelly, T., Nuckolls, G., and Turner, C. (1988). Focal adhesions: trans-membrane junctions between the extracellular matrix and the cytoskeleton. Annu. Rev. Cell Biol. *4*, 487–525.

Calalb, M. B., Poste, T. R., and Hanks, S. K. (1994). Tyrosine phosphorylation of focal adhesion kinase at sites in the catalytic domain regulates kinase activity: a role for *src* family kinases. Mol. Cell. Biol. *15*, 954–963.

Castle, V. P., Ou, X., O'Rourke, K., and Dixit, V. M. (1993). High level thrombospondin 1 expression in two NIH 3T3 cloned lines confers serum and anchorage-independent growth. J. Biol. Chem. *268*, 2899–2903.

Chong, A. S. F., Boussy, I. A., Graf, L. H., and Scuderi, P. (1992). Stimulation of IFN-γ, TNF-α and TNF-β secretion in IL-2 activated T cells: costimulatory roles for LFA-1, LFA-2, CD44, and CD45 molecules. Cell Immunol. *144*, 69–79.

Damsky, C., and Werb, Z. (1992). Signal transduction by integrin receptors for extracellular matrix: cooperative processing of extracellular information. Curr. Opin. Cell Biol. *4*, 772–781.

Egan, S. E., Wright, J. A., Jarolim, L., Yanagihara, K., Bassin, R. H., and Greenberg, A. H. (1987). Transformation by oncogenes encoding protein kinases induces the metastatic phenotype. Science *238*, 202–205.

Entwistle, J., Zhang, S., Yang, B., Wong, C., Qun, L., Hall, C., A, J., Mowat, M., Greenberg, A. H., and Turley, E. A. (1995). Characterization of the murine gene encoding the hyaluronan receptor RHAMM. Gene, in press.

Evans, S. C., Lopez, L. C., and Shur, B. D. (1993). Dominant negative mutation in cell surface β1, 4-galactosyltransferase inhibits cell-cell and cell-matrix interactions. J. Cell Biol. *120*, 1045–1057.

Fraser, R., and Laurent, T. (1993). Hyaluronate. FASEB J. *6*, 2397–2404.

Giancotti, F. G., and Ruoslahti, E. (1990). Elevated levels of the $\alpha_5\beta_1$ fibronectin receptor suppress the transformed phenotype of Chinese hamster ovary cells. Cell *60*, 849–859.

Gunning, P., Leavitt, J., Muscat, G., Ng, S. Y., and Kedes, L. (1987). A human β acton expression vector system directs high-level accumulation of antisense transcripts. Proc. Natl. Acad. Sci. USA *84*, 4831–4835.

Günthert, U. (1993). CD44: a multitude of isoforms with diverse functions. Curr. Topics Microbiol. Immunol. *184*, 47–63.

Günthert, U., Hofmann, M., Rudy, W., Reber, S., Zoller, M., Haubmann, I., Matzku, S., Wenzel, A., Ponta, H., and Herrlich, P. (1991). A new variant of glycoprotein CD44 confers metastatic potential to rat carcinoma cells. Cell *65*, 13–24.

Hall, C. L., Wang, C., Lange, L. A., and Turley, E. A. (1994). Hyaluronan and the hyaluronan receptor RHAMM promote focal adhesion turnover and transient tyrosine kinase activity. J. Cell Biol. *126*, 575–588.

Hardwick, C., Hoare, K., Owens, R., Hohn, H. P., Hook, M., Moore, D., Cripps, V., Austen, L., Nance, D. M., and Turley, E. A. (1992). Molecular cloning of a novel hyaluronan receptor that mediates tumor cell motility. J. Cell Biol. *117*, 1343–1350.

Hiro, D., Ito, A., Matsuta, K., and Mori, Y. (1986). Hyaluronic acid is an endogenous inducer of interleukin-1 production by human monocytes and rabbit macrophages. Biochem. Biophys. Res. Commun. *140*, 715–722.

Hoare, K., Savani, R. C., Wang, C., Yang, B., and Turley, E. A. (1993). Identification of hyaluronan binding proteins using a biotinylated hyaluronan probe. Connect. Tissue Res. *30*, 117–126.

Howlett, A. R., and Bissell, M. J. (1993). The influence of tissue microenvironment (stroma and extracellular matrix) in the development and function of mammary epithelium. Epithel. Cell Biol. *2*, 79–89.

Hynes, R. O. (1992). Integrins: versatility, modulation, and signaling in cell adhesion. Cell *69*, 11–25.

Jones, P. C., Schmidhauser, C., and Bissell, M. J. (1993). Regulation of gene expression and cell function by extracellular matrix. Crit. Rev. Eukaryot. Gene Expr. *3*, 137–154.

Juliano, R. C., and Haskill, S. (1993). Signal transduction from the extracellular matrix. J. Cell Biol. *120*, 577–585.

Kariko, K., Kuo, A., Boyd, D., Okada, S. S., Cines, D. B., and Barnathan, E. S. (1993). Overexpression of urokinase receptor increases invasion without altering cell migration in human osteosarcoma cell line. Cancer Res. *53*, 3109–3117.

Kashles, O., Yarden, Y., Fischer, R., Ullrich, A., and Schlessinger, J. (1991). A dominant negative mutation suppresses the function of normal epidermal growth factor receptors by hetero dimerization. Mol. Cell. Biol. *11*, 1454–1463.

Khokha, R., Zimmer, M. J., Graham, C. H., Lala, P. K., and Waterhouse, P. (1992). Suppression of invasion by inducible expression of tissue inhibitor of metalloproteinase-1 (TIMP-1) in B16-F10 melanoma cells. J. Natl. Cancer Inst. *84*, 1017–1022.

Klewes, L., Turley, E. A., and Prehm, P. (1993). The hyaluronate synthase from a eukaryotic cell line. Biochem. J. *290*, 791–795.

Knudson, C. B., and Knudson, W. (1993). Hyaluronan-binding proteins in development, tissue homeostasis and disease. FASEB J. *7*, 1233–1241.

Leibl, E. C., and Martin, G. S. (1992). Intracellular targeting of $pp60^{src}$ expression: localization of v-src to adhesion plagues is sufficient to transform chicken embryo fibroblasts. Oncogene *7*, 2417–2428.

Lin, C. Q., and Bissell, M. J. (1993). Multi-faceted regulation of cell differentiation by extracellular matrix. FASEB J. *7*, 735–743.

Lo, S. H., and Chen, L. B. (1994). Focal adhesion as a signal transduction organelle. Cancer Metastasis Rev. *13*, 9–24.

Matsumoto, K., Matsumoto, K., Nakamura, T., and Kramer, R. H. (1994). Hepatocyte growth factor/scatter factor induces tyrosine phosphorylation of focal adhesion kinase ($p125^{FAK}$) and promotes migration and invasion by oral squamous cell carcinoma cells. J. Biol. Chem. *269*, 31807–31813.

McGlade, J., Brunkhorst, B., Anderson, D., Mbamalu, G., Settleman, J., Dedhar, S., Rozakis-Adcosk, M., Chen, L. B., and Pawson, T. (1993). The N-terminal region of GAP regulates cytoskeletal structure and cell adhesion. EMBO J. *12*, 3073–3081.

Murphy-Ullrich, J. E., and Hook, M. (1989). Thrombospondin modulates focal adhesions in endothelial cells. J. Cell Biol. *109*, 1309–1312.

Murphy-Ullrich, J. E., Lightner, V. A., Aukhil, I., Yan, Y. Z., Erickson, H. P., and Hook, M. (1991). Focal adhesion integrity is downregulated by the alternatively spliced domain of human tenascin. J. Cell Biol. *115*, 1127–1136.

Noble, P. W., Lake, F. R., Henson, P. M., and Riches, D. W. H. (1993). Hyaluronate activation of CD44 induces insulin-like growth factor expression by a tumor necrosis factor α dependent mechanism in murine macrophages. J. Clin. Invest. *91*, 2368–2377.

Qian, F., Vaux, D. L., and Weissman, F. L. (1994). Expression of the

integrin α4β1 on melanoma cells can inhibit the invasive stage of metastasis formation. Cell *77*, 335–347.

Ratner, S. (1992). Lymphocyte migration through extracellular matrix. Invasion Metastasis *12*, 82–100.

Rodriguez-Fernández, J. L. R., Geiger, B., Salomon, D., and Ben-Ze'ev, A. (1993). Suppression of vinculin expression by antisense transfection confers changes in cell morphology, motility and anchorage-dependent growth of 3T3 cells. J. Cell Biol. *122*, 1285–1294.

Ruoslahti, E., Noble, N. A., Kagami, S., and Border, W. A. (1994). Integrins. Kidney Int. (Suppl. 44) *45*, S17–S22.

Saarialho-Kere, U. K., Kovacs, S. O., Pentland, A. P., Olevid, J. E., Welgus, H. G., and Parks, W. C. (1993). Cell-matrix interactions modulate interstitial collagenase expression by human keratinocyte actively involved in wound healing. J. Clin. Invest. *92*, 2858–2866.

Samuel, S. K., Hurta, R. A. R., Spearman, M. A., Wright, J. A., Turley, E. A., and Greenberg, A. H. (1993). TGF-β_1 stimulation of cell locomotion utilizes the hyaluronan receptor RHAMM and hyaluronan. J. Cell Biol. *123*, 749–758.

Schaller, M. D., and Parsons, J. T. (1994). Focal adhesion kinase and associated proteins. Curr. Opin. Cell Biol. *6*, 705–710.

Schaller, M. D., Borgman, C. A., Cobb, B. S., Vines, R. R., Reynolds, A. B., and Parsons, J. T. (1992). pp125^{FAK}, a structurally distinctive protein-tyrosine kinase associated with focal adhesions. Proc. Natl. Acad. Sci. USA *89*, 5192–5196.

Schlaepfer, D. D., Hanks, S. K., Hunter, J., and van der Geer, P. (1994). Integrin-mediated signal transduction linked to Ras pathway by GRB2 binding to focal adhesion kinase. Nature *372*, 786–791.

Schwartz, M. A. (1993). Signalling by integrins: implications for tumorigenesis. Cancer Res. *53*, 1503–1506.

Shapiro, S., Doyle, G. A. D., Parks, W. C., Ley, T. J., and Welgus, H. G. (1993). Molecular mechanisms regulating the production of collagenase β TIMP in U937 cells: evidence for involvement of delayed transcriptional activation and enhanced mRNA stability. Biochemistry *32*, 4286–4292.

Stetler-Stevenson, W. G., Aznavoorian, S., and Liotta, L. A. (1993). Tumor cell interactions with the extracellular matrix during invasion and metastasis. Am. Rev. Cell Biol. *9*, 541–573.

Sy, M. S., Guo, Y. J., and Stamenkovic, I. (1991). Distinct effects of two CD44 isoforms on tumor growth *in vivo*. J. Exp. Med. *174*, 859–866.

Turley, E. A. (1992). Hyaluronan and cell locomotion. Cancer Metastasis Rev. *11*, 21–30.

Turley, E. A., and Tretiak, M. (1984). Glycosominoglycans produced by murine melanoma variants *in vivo* and *in vitro*. Cancer Res. *45*, 5098–5105.

Turley, E. A., Tretiak, M., and Tanguay, K. (1987). Effect of glycosaminoglycans and enzymes on the integrity of human placental amnion as a barrier to cell invasion. J. Natl. Cancer Inst. *78*, 787–795.

Turley, E. A., Austen, L., Vandeligt, K., and Moore, D. (1991). Hyaluronan and a cell associated hyaluronan binding protein regulate the locomotion of *ras*-transformed cells. J. Cell Biol. *112*, 1041–1047.

Varner, J. A., Fisher, M. H., and Juliano, R. L. (1992). Ectopic expression of integrin α5β1 suppresses *in vitro* growth and tumorigenicity of human colon carcinoma cells. Mol. Biol. Cell *3*, 232a.

Wehrle-Haller, B., and Chiquet, M. (1993). Dual function of tenascin: simultaneous promotion of neurite growth and inhibition of glial migration. J. Cell Sci. *106*, 597–610.

Werb, Z., Tremble, P. M., Behrendtsen, E., Crowley, E., and Damsky, C. H. (1989). Signal transduction through the fibronectin receptor induces collagenase and stromelysin gene expression. J. Cell Biol. *109*, 877–889.

Woods, A., and Couchman, J. R. (1988). Focal adhesions and cell matrix interactions. Collagen Cell. Res. *8*, 155–182.

Yang, B., Yang, B., Savani, R. C., and Turley, E. A. (1994). Identification of a common hyaluronan binding motif in the hyaluronan proteins RHAMM, CD44 and link protein. EMBO J. *13*, 286–296.

Zachary, I., and Rozengurt, E. (1992). Focal adhesion kinase (p125^{FAK}): a point of convergence in the action of neuropeptides, integrins, and oncogenes. Cell *71*, 891–894.